

Memory effect on energy losses of charged particles moving parallel to solid surface

C.M. Kwei^{a,*}, Y.H. Tu^a, Y.H. Hsu^a, C.J. Tung^b

^a Department of Electronics Engineering, National Chiao Tung University, Hsinchu 300, Taiwan

^b Department of Nuclear Science, National Tsing Hua University, Hsinchu 300, Taiwan

Received 16 June 2005; received in revised form 22 August 2005

Available online 26 October 2005

Abstract

Theoretical derivations were made for the induced potential and the stopping power of a charged particle moving close and parallel to the surface of a solid. It was illustrated that the induced potential produced by the interaction of particle and solid depended not only on the velocity but also on the previous velocity of the particle before its last inelastic interaction. Another words, the particle kept a memory on its previous velocity, v_0 , in determining the stopping power for the particle of velocity v . Based on the dielectric response theory, formulas were derived for the induced potential and the stopping power with memory effect. An extended Drude dielectric function with spatial dispersion was used in the application of these formulas for a proton moving parallel to Si surface. It was found that the induced potential with memory effect lay between induced potentials without memory effect for constant velocities v_0 and v . The memory effect was manifest as the proton changes its velocity in the previous inelastic interaction. This memory effect also reduced the stopping power of the proton. The formulas derived in the present work can be applied to any solid surface and charged particle moving with arbitrary parallel trajectory either inside or outside the solid.

© 2005 Elsevier B.V. All rights reserved.

PACS: 78.20.Bh; 78.70.-g

Keywords: Memory effect; Surface excitation; Inelastic interaction

1. Introduction

When a charged particle moves close and parallel to the surface of a solid, induced potential is produced due to the interaction of particle and solid. This potential is then acted on the particle resulting to a stopping power. Theoretical derivations of the induced potential and the stopping power were previously made [1–4] for a constant velocity, v_0 , of the particle until it experienced an inelastic interaction. After the interaction, the particle changed its velocity to v and continued to interact with the solid. For a second inelastic interaction, it was generally assumed that a new induced

potential, dependent only on v but not on v_0 , was generated. This new potential then determined the stopping power acting on the particle of velocity v . In the present work, the induced potential and stopping power for the second inelastic interaction were derived using image charges and dielectric response functions. It was found that the particle previous velocity v_0 had also an effect on the second inelastic interaction. Another words, the particle kept a memory on its previous velocity, v_0 , in determining the stopping power for the particle of velocity v .

The response of solid to a charged particle moving close and parallel to the surface may be characterized by its surface loss-function, $\text{Im}[-1/(\epsilon + 1)]$, where ϵ is the dielectric function of the solid and $\text{Im}[\]$ denotes the imaginary part. A sum-rule-constrained extended Drude dielectric function with spatial dispersion [5] was established with parameters determined from optical data. Previously, this dielectric

* Corresponding author. Tel.: +886 3 5712121x54136; fax: +886 3 5727300.

E-mail addresses: cmkwei@mail.nctu.edu.tw, cmkwei@cc.nctu.edu.tw (C.M. Kwei).

function was applied to the interface [6–8] and overlayer systems [3,9,10] for a charged particle without memory effect. With the consideration of memory effect, we applied this dielectric function in this work. The induced potential was then derived by solving Poisson equations in Fourier space by a method of image charges which satisfied the boundary conditions. The stopping power was then constructed from the derivative of the induced potential at particle position. Calculations were made using these formulas for a proton moving parallel to Si surface. Results were analyzed for the dependences of the induced potential and stopping power on proton velocities before and after the last inelastic interaction, the distance from surface, and the distance from previous inelastic interaction. Finally, the calculated results with memory effect were compared with the corresponding results without memory effect.

2. Theory

Fig. 1 illustrates the problem studied in the present work. A particle of charge q , velocity \vec{v}_0 and energy E_0 moves parallel to the interface of two media of dielectric functions $\varepsilon_1(\vec{k}, \omega)$ and $\varepsilon_2(\vec{k}, \omega)$. The interface is located at $z = 0$, with z -axis perpendicular to the interface plane and directed from $\varepsilon_1(\vec{k}, \omega)$ to $\varepsilon_2(\vec{k}, \omega)$. The particle is moving along y -direction at a distance D above the interface. At the moment $t = 0$, the particle experiences an inelastic interaction which changes particle velocity and energy to \vec{v} and E . Assuming the particle continues to move along the same direction, the induced potential at $t > 0$ is of special interest here. For $z > 0$, the scalar potential is produced by the particle and a fictitious charge at $z < 0$ near the interface. For

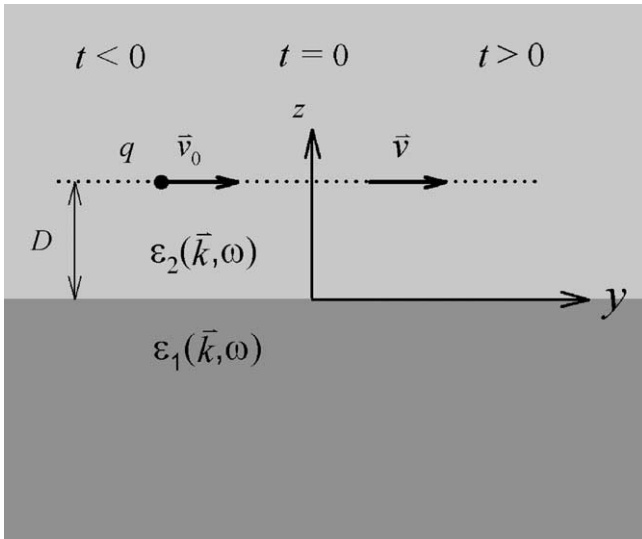


Fig. 1. A sketch of the problem studied in the present work. A particle of charge q , velocity \vec{v}_0 moves parallel to the interface of two media of dielectric functions $\varepsilon_1(\vec{k}, \omega)$ and $\varepsilon_2(\vec{k}, \omega)$. The interface is located at $z = 0$ and the particle is moving along y -direction at a distance D above the interface. At time $t = 0$, the particle experiences an inelastic interaction which changes particle velocity to v . Special interest is on the induced potential and the stopping power at $t > 0$.

$z < 0$, the potential is produced by a fictitious charge at particle position and by another fictitious charge at $z > 0$ near the interface. These fictitious charges should be established using boundary conditions that are satisfied at the interface. Thus the Poisson equations in Fourier space are

$$\varphi_1(\vec{k}, \omega) = \frac{4\pi}{k^2 \varepsilon_1(\vec{k}, \omega)} \left[\rho(\vec{k}, \omega) + \rho_f(\vec{Q}, \omega) \right] \quad (1)$$

for $z < 0$ and

$$\varphi_2(\vec{k}, \omega) = \frac{4\pi}{k^2 \varepsilon_2(\vec{k}, \omega)} \left[\rho(\vec{k}, \omega) - \rho_f(\vec{Q}, \omega) \right] \quad (2)$$

for $z > 0$, where $\vec{k} = (k_x, k_y, k_z) = (\vec{Q}, k_z)$ is the momentum transfer and ω is the energy transfer. The Fourier transform of the charge density distribution of the particle

$$\rho(\vec{r}, t) = q\delta(x)\delta(z-D)[\delta(y-v_0t)\Theta(-t) + \delta(y-vt)\Theta(t)] \quad (3)$$

is given by

$$\rho(\vec{k}, \omega) = qe^{-ik_z D} \left[\int_{-\infty}^0 e^{i(\omega-k_y v_0)\tau} d\tau + \int_0^{\infty} e^{i(\omega-k_y v)\tau} d\tau \right], \quad (4)$$

where $\delta()$ and $\Theta()$ are the delta- and step-functions, respectively. To satisfy the boundary conditions at the interface, the fictitious charge in Fourier space is given by

$$\rho_f(\vec{Q}, \omega) = \frac{\int_{-\infty}^{\infty} \frac{\rho(\vec{k}, \omega)}{k^2} \left[\frac{1}{\varepsilon_2(\vec{k}, \omega)} - \frac{1}{\varepsilon_1(\vec{k}, \omega)} \right] dk_z}{\int_{-\infty}^{\infty} \frac{1}{k^2} \left[\frac{1}{\varepsilon_2(\vec{k}, \omega)} + \frac{1}{\varepsilon_1(\vec{k}, \omega)} \right] dk_z}. \quad (5)$$

Combining Eqs. (4) and (5), one gets

$$\rho_f(\vec{Q}, \omega) = q \left[\int_{-\infty}^0 e^{i(\omega-k_y v_0)\tau} d\tau + \int_0^{\infty} e^{i(\omega-k_y v)\tau} d\tau \right] \times \left[\frac{\frac{1}{\varepsilon_2(D, \vec{Q}, \omega)} - \frac{1}{\varepsilon_1(D, \vec{Q}, \omega)}}{\frac{1}{\varepsilon_2(\vec{Q}, \omega)} + \frac{1}{\varepsilon_1(\vec{Q}, \omega)}} \right], \quad (6)$$

where the effective dielectric function is given by

$$\frac{1}{\bar{\varepsilon}_L(D, \vec{Q}, \omega)} = \frac{1}{2\pi} \int_{-\infty}^{\infty} \frac{e^{-ik_z D}}{k^2 \varepsilon_L(\vec{k}, \omega)} dk_z \quad (7)$$

for $L = 1$ and 2 and $\bar{\varepsilon}_L(\vec{Q}, \omega) = \bar{\varepsilon}_L(0, \vec{Q}, \omega)$.

Substituting Eqs. (4)–(7) into Eqs. (1) and (2), one obtains the scalar potentials in Fourier space, i.e. $\varphi_1(\vec{k}, \omega)$ and $\varphi_2(\vec{k}, \omega)$. The induced potentials in Fourier space, $\varphi_1^{\text{ind}}(\vec{k}, \omega)$ and $\varphi_2^{\text{ind}}(\vec{k}, \omega)$, are then obtained by removing the vacuum potential of the particle from scalar potentials. One gets

$$\varphi_1^{\text{ind}}(\vec{k}, \omega) = \frac{4\pi}{k^2} \left(\frac{1}{\varepsilon_1(\vec{k}, \omega)} - 1 \right) \rho(\vec{k}, \omega) + \frac{4\pi}{k^2 \varepsilon_1(\vec{k}, \omega)} \rho_f(\vec{Q}, \omega) \quad (8)$$

for $z < 0$ and

$$\varphi_2^{\text{ind}}(\vec{k}, \omega) = \frac{4\pi}{k^2} \left(\frac{1}{\varepsilon_2(\vec{k}, \omega)} - 1 \right) \rho(\vec{k}, \omega) - \frac{4\pi}{k^2 \varepsilon_2(\vec{k}, \omega)} \rho_f(\vec{Q}, \omega) \quad (9)$$

for $z > 0$. If the particle is moving in vacuum, i.e. $\varepsilon_2 = 1$, one gets

$$\varphi_2^{\text{ind}}(\vec{k}, \omega) = -\frac{4\pi q}{k^2} \left[\int_{-\infty}^0 e^{i(\omega - k_y v_0)\tau} d\tau + \int_0^{\infty} e^{i(\omega - k_y v)\tau} d\tau \right] \times \left[\frac{\frac{1}{\varepsilon_2(D, \vec{Q}, \omega)} - \frac{1}{\varepsilon_1(D, \vec{Q}, \omega)}}{\frac{1}{\varepsilon_2(\vec{Q}, \omega)} + \frac{1}{\varepsilon_1(\vec{Q}, \omega)}} \right] \quad (10)$$

after substituting Eq. (6) into Eq. (9). Since ε is weakly dependent on k_z than the rest of k components, one may assume $\varepsilon(\vec{k}, \omega) = \varepsilon(\vec{Q}, \omega)$. This assumption was previously adopted by Yubero et al. [11,12] in the analyses of REELS spectra and by Kwei et al. [9,13] in the calculations of electron elastic backscattering spectra. Using this assumption, Eq. (7) becomes

$$\frac{1}{\varepsilon_L(D, \vec{Q}, \omega)} \approx \frac{e^{-|D|Q}}{2Q} \frac{1}{\varepsilon_L(\vec{Q}, \omega)}. \quad (11)$$

Applying the relation [14] for the product of the step-function and the delta-function, i.e. $\Theta(s)\delta(s) = \frac{1}{2}\delta(s)$, Eq. (10) may be written as

$$\varphi_2^{\text{ind}}(\vec{k}, \omega) = -\frac{4\pi^2 q}{k^2} [\delta(\omega - k_y v_0) + \delta(\omega - k_y v)] \times \left[\frac{e^{-|D|Q} \frac{\varepsilon_1(\vec{Q}, \omega) - 1}{\varepsilon_1(\vec{Q}, \omega) + 1}}{\varepsilon_1(\vec{Q}, \omega) + 1} \right]. \quad (12)$$

Applying $\varepsilon(\vec{Q}, \omega) = \varepsilon(Q, \omega)$ and $\varepsilon(Q, -\omega) = \varepsilon^*(Q, \omega)$, the induced potential in real space is obtained by an inverse Fourier transform as

$$\begin{aligned} \varphi_2^{\text{ind}}(\vec{r}, t) &= \frac{-q}{\pi^2} \int_0^{\infty} d\omega \int_0^{\infty} dk \int_0^{\pi} \sin \theta d\theta \\ &\times \int_0^{2\pi} d\phi \delta(\omega - k_y v_0) e^{-|D|Q} \\ &\times \cos(k_z z) \text{Re} \left[\frac{\varepsilon_1(Q, \omega) - 1}{\varepsilon_1(Q, \omega) + 1} e^{i(k_x x + k_y y - \omega t)} \right] \\ &+ \frac{-q}{\pi^2} \int_0^{\infty} d\omega \int_0^{\infty} dk \int_0^{\pi} \sin \theta d\theta \\ &\times \int_0^{2\pi} d\phi \delta(\omega - k_y v) e^{-|D|Q} \\ &\times \cos(k_z z) \text{Re} \left[\frac{\varepsilon_1(Q, \omega) - 1}{\varepsilon_1(Q, \omega) + 1} e^{i(k_x x + k_y y - \omega t)} \right]. \quad (13) \end{aligned}$$

Expanding the δ -function according to

$$\begin{aligned} \delta(\omega - kv \sin \theta \sin \phi) &= \frac{1}{\sqrt{(kv \sin \theta)^2 - \omega^2}} \\ &\times \left\{ \delta\left(\phi - \sin^{-1} \frac{\omega}{kv \sin \theta}\right) \right. \\ &\left. + \delta\left[\phi - \left(\pi - \sin^{-1} \frac{\omega}{kv \sin \theta}\right)\right] \right\}, \quad (14) \end{aligned}$$

and applying the conservation relations of energy and momentum, it gives

$$\begin{aligned} \varphi_2^{\text{ind}}(\vec{r}, t) &= \frac{-2q}{\pi^2} \int_0^E d\omega \int_{k_{\min}}^{k_{\max}} dk \int_{\frac{\omega}{v_0}}^{\frac{\omega}{v}} dQ \frac{Q}{k} \\ &\times \frac{\cos\left(z\sqrt{k^2 - Q^2}\right)}{\sqrt{k^2 - Q^2} \sqrt{(Qv_0)^2 - \omega^2}} e^{-|D|Q} \\ &\times \cos\left(\frac{x}{v_0} \sqrt{(Qv_0)^2 - \omega^2}\right) \left\{ \text{Re} \left[\frac{\varepsilon_1(Q, \omega) - 1}{\varepsilon_1(Q, \omega) + 1} \right] \right. \\ &\times \cos\left(\frac{\omega}{v_0}(y - v_0 t)\right) - \text{Im} \left[\frac{\varepsilon_1(Q, \omega) - 1}{\varepsilon_1(Q, \omega) + 1} \right] \\ &\times \sin\left(\frac{\omega}{v_0}(y - v_0 t)\right) \left. \right\} + \frac{-2q}{\pi^2} \int_0^E d\omega \int_{k_{\min}}^{k_{\max}} dk \\ &\times \int_{\frac{\omega}{v}}^{\frac{\omega}{v_0}} dQ \frac{Q}{k} \frac{\cos\left(z\sqrt{k^2 - Q^2}\right)}{\sqrt{k^2 - Q^2} \sqrt{(Qv)^2 - \omega^2}} e^{-|D|Q} \\ &\times \cos\left(\frac{x}{v} \sqrt{(Qv)^2 - \omega^2}\right) \left\{ \text{Re} \left[\frac{\varepsilon_1(Q, \omega) - 1}{\varepsilon_1(Q, \omega) + 1} \right] \right. \\ &\times \cos\left(\frac{\omega}{v}(y - vt)\right) - \text{Im} \left[\frac{\varepsilon_1(Q, \omega) - 1}{\varepsilon_1(Q, \omega) + 1} \right] \\ &\times \sin\left(\frac{\omega}{v}(y - vt)\right) \left. \right\}, \quad (15) \end{aligned}$$

where $Q = k \sin \theta$, $k_{\max} = \sqrt{2ME} + \sqrt{2ME - 2M\omega}$, $k_{\min} = \sqrt{2ME} - \sqrt{2ME - 2M\omega}$ and M is the mass of the particle.

The stopping power is related to the derivative of $\varphi_2^{\text{ind}}(\vec{r}, t)$ at the position of particle, i.e. $\vec{r}_p = (x_p, y_p, z_p) = (0, vt, D)$, for $t > 0$. One finds

$$\begin{aligned} -\frac{dW}{ds}(y_p) &= \frac{2q^2}{\pi^2 v_0} \int_0^E d\omega \int_{k_{\min}}^{k_{\max}} dk \\ &\times \int_{\frac{\omega}{v_0}}^{\frac{\omega}{v}} dQ \frac{Q}{k} \frac{\omega \cos\left(|D|\sqrt{k^2 - Q^2}\right)}{\sqrt{k^2 - Q^2} \sqrt{(Qv_0)^2 - \omega^2}} e^{-|D|Q} \\ &\times \left\{ \text{Re} \left[\frac{\varepsilon_1(Q, \omega) - 1}{\varepsilon_1(Q, \omega) + 1} \right] \sin\left(\frac{\omega}{v_0 v}(v - v_0)y_p\right) \right. \\ &\left. + \text{Im} \left[\frac{\varepsilon_1(Q, \omega) - 1}{\varepsilon_1(Q, \omega) + 1} \right] \cos\left(\frac{\omega}{v_0 v}(v - v_0)y_p\right) \right\} \\ &+ \frac{2q^2}{\pi^2 v} \int_0^E d\omega \int_{k_{\min}}^{k_{\max}} dk \int_{\frac{\omega}{v}}^{\frac{\omega}{v_0}} dQ \frac{Q}{k} \\ &\times \frac{\omega \cos\left(|D|\sqrt{k^2 - Q^2}\right)}{\sqrt{k^2 - Q^2} \sqrt{(Qv)^2 - \omega^2}} e^{-|D|Q} \text{Im} \left[\frac{\varepsilon_1(Q, \omega) - 1}{\varepsilon_1(Q, \omega) + 1} \right]. \quad (16) \end{aligned}$$

Letting $v = v_0$, Eqs. (15) and (16) reduce to the same formulas for the induced potential and the stopping power that were derived without memory effect by Kwei et al. [3]. Note that the stopping power in Eq. (16) is y_p dependent. Thus the stopping power with memory effect may be obtained by an average over all particles paths

$$-\frac{dW}{ds} = \frac{\int_0^\infty \frac{y_p}{\lambda} e^{-y_p/\lambda} \left(-\frac{dW}{ds}(y_p)\right) dy_p}{\int_0^\infty \frac{y_p}{\lambda} e^{-y_p/\lambda} dy_p}, \quad (17)$$

where $\frac{y_p}{\lambda} e^{-y_p/\lambda}$ is the probability that the particle encounters an inelastic interaction in the distance y_p [11,15] and λ is the inelastic mean free path.

3. Results and discussion

Fig. 2 shows plots of the real and imaginary parts of the surface response function, i.e. $[\varepsilon_1(0, \omega) - 1]/[\varepsilon_1(0, \omega) + 1]$, for vacuum–Si interface as a function of energy transfer ω . The solid curves are fitting results obtained in the present work. The dotted curves are corresponding data deduced from optical data [16]. It is seen that the calculated results are in good agreement with measured data.

The induced potential for a proton moving parallel to the surface of Si was calculated using Eq. (15). Results at the position of proton for $y_p = 5$ a.u., $v_0 = 10$ a.u. and $D = 1$ a.u. are plotted in Fig. 3 (solid curve) as a function of proton velocity v . These results are compared with corresponding data without the memory effect (dotted curve), where the abscissa v here may also be interpreted as v_0 . It reveals that both curves show a dip around $v = 1.5$ a.u. The existence of a dip was also shown for a proton moving parallel to Al surface in the plasmon-pole dielectric function model [2]. As indicated in the figure, the magnitude of induced potential decreases with increasing velocity for

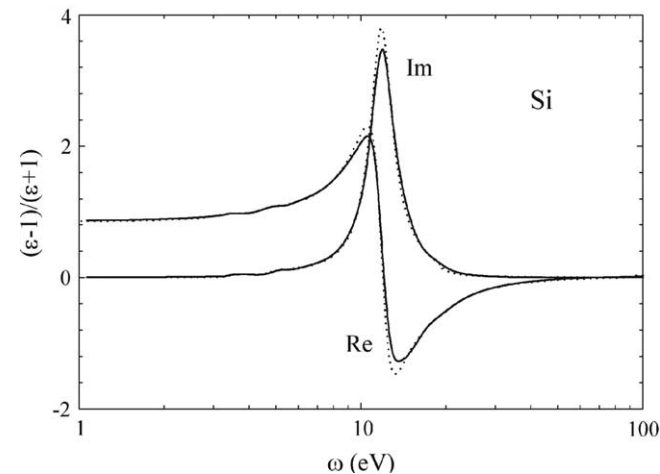


Fig. 2. A plot of the real and imaginary parts of the surface response function, $[\varepsilon_1(0, \omega) - 1]/[\varepsilon_1(0, \omega) + 1]$, for vacuum–Si interface as a function of energy transfer ω . The solid curves are fitting results using the extended Drude dielectric function. The dotted curves are results deduced from the optical data [16].

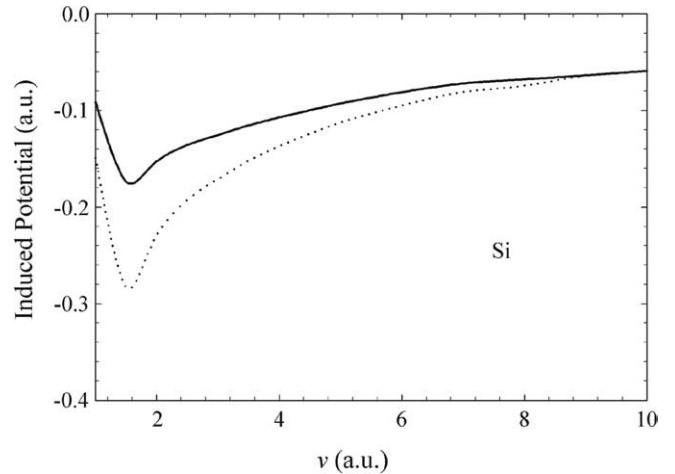


Fig. 3. The induced potential for a proton moving parallel to the surface of Si. Results (solid curve) are plotted at proton position for $y_p = 5$ a.u., $v_0 = 10$ a.u. and $D = 1$ a.u. as a function of proton velocity v . Corresponding results without the memory effect are plotted (dotted curve) for a comparison.

velocities larger than the dip velocity and increases with increasing velocity for velocities smaller than the dip velocity. Note that there is a significant difference between solid and dotted curves. At $v = 2$ a.u., for instance, solid and dotted curves correspond to $v_0 = 10$ a.u. (with memory effect) and $v_0 = 2$ a.u. (without memory effect), respectively. Since the velocity change, $v_0 - v$, in the solid curve is large so that the difference between solid and dotted curves is also large. At $v = 8$ a.u., on the other hand, solid and dotted curves correspond to $v_0 = 10$ a.u. and 8 a.u., respectively. In this case, the velocity change in the solid curve is small so that the difference is also small. Thus the difference in induced potentials calculated with and without the memory effect increases with increasing velocity change in the previous inelastic interaction when $v \geq 1.5$ a.u. When $v < 1.5$ a.u., however, the difference decreases with increasing velocity change.

The induced potential shown in Fig. 3 is at proton position, i.e. $y = y_p$. Fig. 4 plots the induced potential at a position, along the trajectory of proton, with a distance $y - y_p$ from the proton for $y_p = 5$ a.u. and $D = 1$ a.u. The solid curve is results (with memory effect) of the induced potential for $v_0 = 5$ a.u. and $v = 3$ a.u. The dotted and dashed curves are corresponding results (without memory effect) for $v = v_0 = 3$ a.u. and 5 a.u., respectively. In all cases, the induced potential exhibits an oscillation behavior over the distance from the proton, a behavior which was also observed by Arista [4]. Note that the induced potential for $v_0 = 5$ a.u. and $v = 3$ a.u. (with memory effect) lies between induced potentials for $v = v_0 = 3$ a.u. and 5 a.u. (without memory effect). This indicates that the induced potential carries a memory effect on proton previous velocity before its last inelastic interaction. A similar plot is made in Fig. 5 for a proton moving at distances $D = 1$

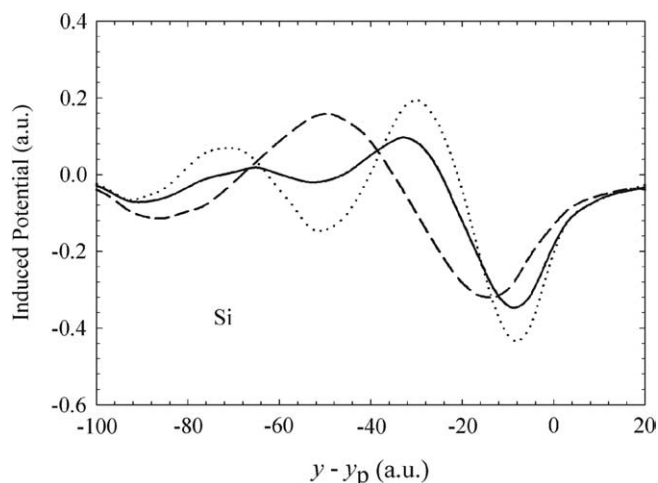


Fig. 4. The induced potential at a distance $y - y_p$ from the proton with $y_p = 5$ a.u. and $D = 1$ a.u. from Si surface. The solid curve is results with the memory effect for $v_0 = 5$ a.u. and $v = 3$ a.u. The dotted and dashed curves are results without the memory effect for $v = v_0 = 3$ a.u. and 5 a.u., respectively.

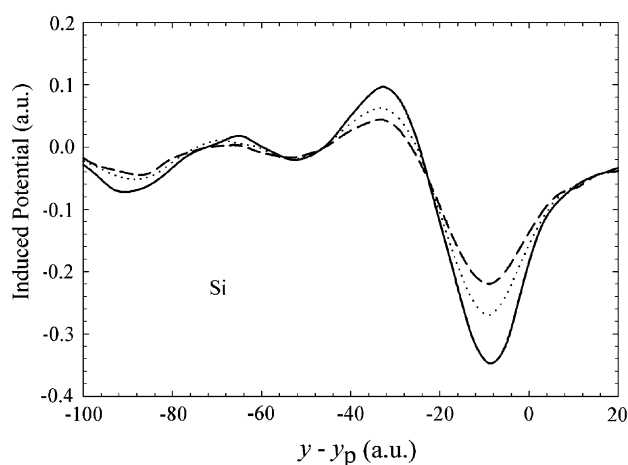


Fig. 5. The induced potential at a distance $y - y_p$ from the proton with $D = 1$ (solid curve), 2 (dotted curve) and 3 a.u. (dashed curve) from Si surface. Here $y_p = 5$ a.u., $v_0 = 5$ a.u. and $v = 3$ a.u.

(solid curve), 2 (dotted curve) and 3 a.u. (dashed curve) from Si surface with $y_p = 5$ a.u., $v_0 = 5$ a.u. and $v = 3$ a.u. It is seen that as D increases the induced potential (absolute value) decreases. This reveals that the induced potential is greater for a proton moving closer to the solid surface.

Fig. 6 shows results of the stopping power for a proton moving parallel to and with at a distance $D = 2$ a.u. from the Si surface. Solid and dotted curves are for $v_0 = 10$ a.u. (with memory effect) and $v_0 = v$ (without memory effect), respectively. The existence of a maximum stopping power at a velocity around 1.5 a.u. was shown. The existence of a maximum was also found for some semi-infinite solids by Arista [4]. A notable difference between solid and dotted curves was shown in the figure. Without the

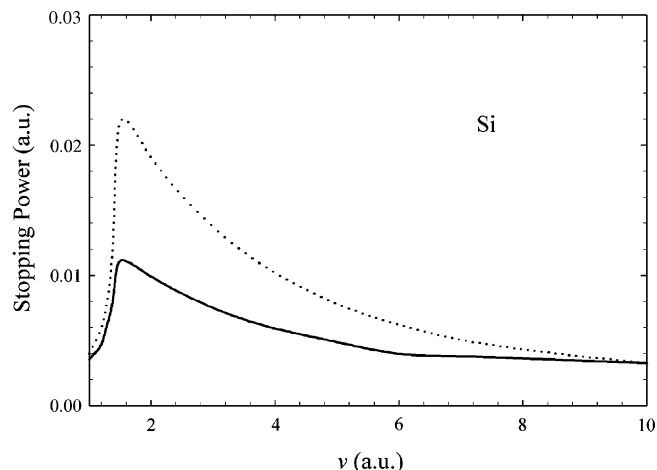


Fig. 6. Results of the stopping power for a proton moving parallel to with a distance $D = 2$ a.u. from the Si surface. Solid and dotted curves are for $v_0 = 10$ a.u. (with memory effect) and $v_0 = v$ (without memory effect), respectively.

memory effect, stopping power is solely determined by v without reference to v_0 . With memory effect, however, the stopping power is affected by both v and v_0 . The memory effect reduced the stopping power for the proton.

4. Conclusions

A theoretical treatment was developed to account for the memory effect on the induced potential and the stopping power for a charged particle moving close and parallel to the surface of a solid. It was illustrated that the particle had a memory on its velocity before the previous inelastic interaction, v_0 , in determining the induced potential and the stopping power for the particle of velocity v . Using the method of image charges, analytical formulas have been derived for the induced potential and the stopping power for particle–surface interactions. An extended Drude dielectric function with spatial dispersion was used in the calculations of the induced potential for a proton moving parallel to Si surface. It was found that the memory effect affected the induced potential and the stopping power. The induced potential with memory effect lay between induced potentials without memory effect for constant velocities v_0 and v . The stopping powers with memory effect were lower than those without memory effect. For a small difference between v_0 and v , which was more probable in an interaction, the memory effect on both induced potential and stopping power was unobvious. Thus, any Monte Carlo simulation using inelastic cross sections without the memory effect in the particle transport near the surface was practically valid. The memory effect, however, should be detected for rare consecutive surface interactions involving large difference between v_0 and v . The formulas derived in the present work can be applied to any solid surface and

charged particle moving with arbitrary parallel trajectory either inside or outside the solid.

Acknowledgement

This research was supported by the National Science Council of the Republic of China under contract no. NSC92-2215-E-009-063.

References

- [1] F.J. García de Abajo, P.M. Echenique, *Phys. Rev. B* 46 (1992) 2663.
- [2] F.J. García de Abajo, P.M. Echenique, *Phys. Rev. B* 48 (1993) 13399.
- [3] C.M. Kwei, S.J. Hwang, Y.C. Li, C.J. Tung, *J. Appl. Phys.* 93 (2003) 9130.
- [4] N.R. Arista, *Phys. Rev. A* 49 (1994) 1885.
- [5] C.M. Kwei, Y.F. Chen, C.J. Tung, J.P. Wang, *Surf. Sci.* 293 (1993) 202.
- [6] C.M. Kwei, C.J. Hung, P. Su, C.J. Tung, *J. Phys. D: Appl. Phys.* 32 (1999) 3122.
- [7] C.M. Kwei, Y.C. Li, *Appl. Surf. Sci.* 238 (2004) 151.
- [8] C.M. Kwei, Y.H. Tu, C.J. Tung, *Nucl. Instr. and Meth. B* 230 (2005) 125.
- [9] C.M. Kwei, S.Y. Chiou, Y.C. Li, *J. Appl. Phys.* 85 (1999) 8247.
- [10] C.M. Kwei, S.S. Tsai, C.J. Tung, *Surf. Sci.* 473 (2001) 50.
- [11] F. Yubero, S. Tougaard, *Phys. Rev. B* 46 (1992) 2486.
- [12] F. Yubero, J.M. Sanz, B. Ramskov, S. Tougaard, *Phys. Rev. B* 53 (1996) 9719.
- [13] C.M. Kwei, C.Y. Wang, C.J. Tung, *Surf. Interf. Anal.* 26 (1998) 682.
- [14] R.F. Hoskins, *Horwood Series in Mathematics and Applications*, Horwood, England, 1999.
- [15] H. Raether, *Springer Tracts in Modern Physics*, Vol. 88, Springer, New York, 1980.
- [16] E.D. Palik (Ed.), *Handbook of Optical Constants of Solids*, Academic Press, New York, 1985.